Applied and Computational Mechanics 9 (2015) 141–148

Negative stiffness in gear contact

L. Půst[a,*], L. Pešek[a], A. Radolfová[a]

[a] *Institute of Thermomechanics, The Czech Academy of Sciences, Dolejškova 5, 182 00 Prague 8, Czech Republic*

Received 5 October 2015; received in revised form 21 December 2015

Abstract

The tooth contact stiffness is very often included in dynamic mathematical models of gear drives. It is an important value for calculation of torsion eigenfrequencies as well as the dynamic properties of the whole transmission systems. Planetary gear drives have several advantages over simple parallel axis gears, especially due to theirs compact design and great torque-to-weight ratio caused by multiple parallel paths. However, the dimensional or mounting errors can cause that some planets have the tendency to take more load than the others. One of the ways how to improve load sharing is the application of flexible planetary pins or by using a free central wheel. However in such cases, the wheels motion is defined in one rotation coordinate and two translation coordinates — tangential and radial. The reaction force at radial change of axis distance is usually neglected. The focus of this contribution is to derive the stiffness of this radial connection and to analyse the influence of radial stiffness on planetary gear dynamics.

Keywords: gearbox, planetary gears, gear trains, contact radial stiffness

1. Introduction

The dynamic analyses of both single-mesh gears systems and multi-mesh planetary gear transmission systems is of fundamental importance for the reduction of noise and vibrations of these very often used mechanical devises [2–4, 10]. A large amount of research work is performed on the lumped-parameter mathematical models [1, 5], where the wheels are supposed to be non-deformable. The elasticity of gear structure is concentrated in springs modelled by discrete translation and rotational stiffness of the shafts, bearings and gears contacts. The properties of discrete mesh stiffness are the most investigated phenomena in gearing modelling. It fluctuates over a mesh cycle, particulary in spur gearing. In helical gearings and in planetary trains, these fluctuations are not so intensive. For the reduction of these fluctuations, some design strategies are applied such as tooth shape modifications or gear geometry adjustments [6]. The improvement of load sharing among the planets is achieved by the use of floating wheels, flexible planetary pins etc. [7–9, 11].

Unfortunately, the application of floating or idle gears causes that the deformations in mesh contact are not only in the direction of tangent to the base circle, but there is also a motion component perpendicular to this tangential motion. Restoring forces at displacement in this radial direction are usually not taken into account and are not respected in mathematical modelling.

The present paper attempts to fill this white place and derive a radial stiffness of gears contact for both external and internal tooth systems. The external gearing has negative stiffness and introduces instability into the gearing system. Added examples show influence of this radial stiffness on the dynamic behaviour of planet trains and of simple parallel gearings.

*Corresponding author. Tel.: +420 266 053 212, e-mail: pust@it.cas.cz.

2. The floating sun gear — one planet stage

Planetary gearboxes have several advantages over the single parallel-axes mechanical gearings, the main one of these is the minimizing of weight of produce at a given power. It is due to splitting of force flow into several planet stages, but the non-ideal mounting, errors in production etc. can cause that the load sharing on all planet stages is very unequal and influences the reliability and service live of the whole product. The correct designs of floating sun gear or flexible pins of planet gears are possible ways how to achieve better performance and reliability. In this paper, the type of gearings to be solved includes the gearbox with fixed planetary carrier and with four planetary subsystems.

However, the structure of such gearing train is more complicated, and as such needs a deeper dynamic analysis. It is not sufficient to solve only a tangential and torsion motion model, but the radial motion has to be given as well. For the sake of simplicity, let us assume that the central sun wheel, planet wheel as well as outer annulus ring wheel have helical gearings. Because this kind of gearings has an essential smaller variation of contact stiffness compared to the direct spur gearings, this stiffness variability is in this study not taken into account.

The tangential forces in tooth contacts are needed for ascertaining of radial stiffness. These contact forces are given by input moment transmitted from the central sun gear to the ring wheel through one planet subsystem. The planetary wheel works as idle gear wheel and the motion of the whole planetary subsystem can be expressed by transversal-torsion dynamic model, described by means of three angles of rotation of ring, planet and sun wheels φ_1, φ_2, φ_3 and of tangential translation of planet wheel x_2.

The dynamic mathematical model of the planetary gearing set is based on several assumptions:

a) Plane motion of all gearing wheels.

b) Rigid wheels, with inertia parameters Θ_1, Θ_2, Θ_3, m_2, m_3.

c) Exact gearings.

d) Compliant planet wheels pivot, stiffness k_c.

e) Entire system is un-damped, linear.

f) Axis of the annulus ring wheel is fixed, wheel can only rotate.

Graphical representation of the kinematic situation is plotted in Fig. 1 and described by the following equations expressing elastic contact deformations in mesh between ring (1) and planet (2) wheels

$$\Delta_1 = \frac{F_1}{k_1} = -r_1\varphi_1 + r_2\varphi_2 - r_4\varphi_4 \tag{1}$$

and in mesh between planet (2) and sun (3) wheels

$$\Delta_2 = \frac{F_2}{k_2} = -x_3 - r_4\varphi_4 - r_2\varphi_2 + r_3\varphi_3. \tag{2}$$

The deformation of planet pin is

$$-x_2 = -\frac{F_4}{k_c} = r_4\varphi_4 \tag{3}$$

and the deformation of sun wheel axis is

$$x_3 = \frac{F_3}{k_3}. \tag{4}$$

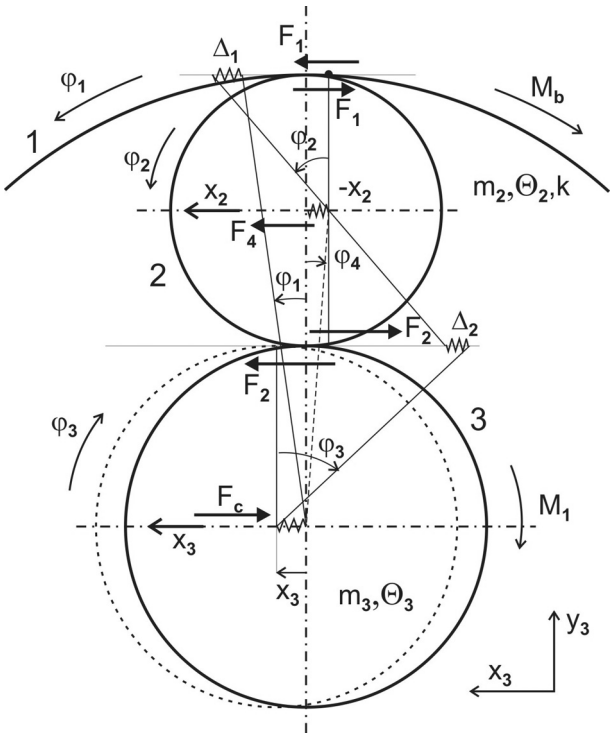

Fig. 1. Kinematic horizontal-rotational situation

These forces or forces of corresponding moments can be used for describing the dynamic properties of the entire gearings train in horizontal-rotational directions. The equations of motion based on the equilibrium of moments are

$$\begin{aligned} \Theta_1\ddot{\varphi}_1 &= F_1 r_1 - M_b, \\ m_2\ddot{x}_2 &= -F_1 - F_2 + F_4, \\ \Theta_2\ddot{\varphi}_2 &= -F_1 r_2 + F_2 r_2, \\ m_3\ddot{x}_3 &= -F_3 + F_2, \\ \Theta_3\ddot{\varphi}_3 &= -F_2 r_3 + M_1, \end{aligned} \tag{5}$$

where we applied Eqs. (3) and (4) for the horizontal motions x_2 and x_3.

The external moments M_1, M_b containing constant component — preload — ascertain forces in gearing contacts, which influence the radial stiffness at mutual radial motions of wheels. Analysis of changes of mesh contact forces at wheel-axis-distance variation is important for the ascertaining of radial forces. This distance variation is connected with the change of pressure angle α as shown in Fig. 2, where the large angle change $\Delta\alpha = 5°$ is used for better clarity. The real angle variation is lower.

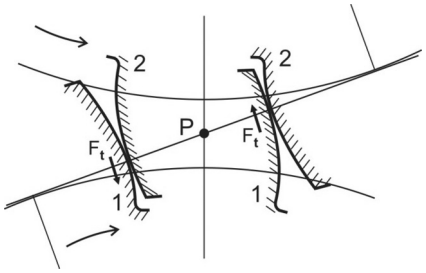

Fig. 2. Friction forces

The tangential component of the mesh contact force increases only insignificantly at the decrease of pressure angle $\Delta\alpha = 1°$, i.e. for the decrease from $\alpha = 25°$ to $\alpha = 24°$, we get $(\cos(25) - \cos(24))/\cos(25) = 0.007\,99$, while the radial component increases $(\sin(25) - \sin(24))/\sin(25) = 0.037\,58$, i.e. nearly 4 %.

The friction forces act also in tooth contacts. These forces are in well-lubricated gearings very low, especially at helical gearings, where the teeth are in contact along the entire line of action. The friction force acts in the dedendum of driver (on line of action in front of pitch point) downwards, in addentum (behind pitch point) the friction forces have opposite directions — Fig. 2, but their moments act always against the revolution of the driver and contribute to the transmission energy losses. In helical gearings with multiple contacts, these moments add together and degrease gearing train efficiency, but the resultant of all friction forces in radial direction is negligible and need not be considered in the equation of vertical motion.

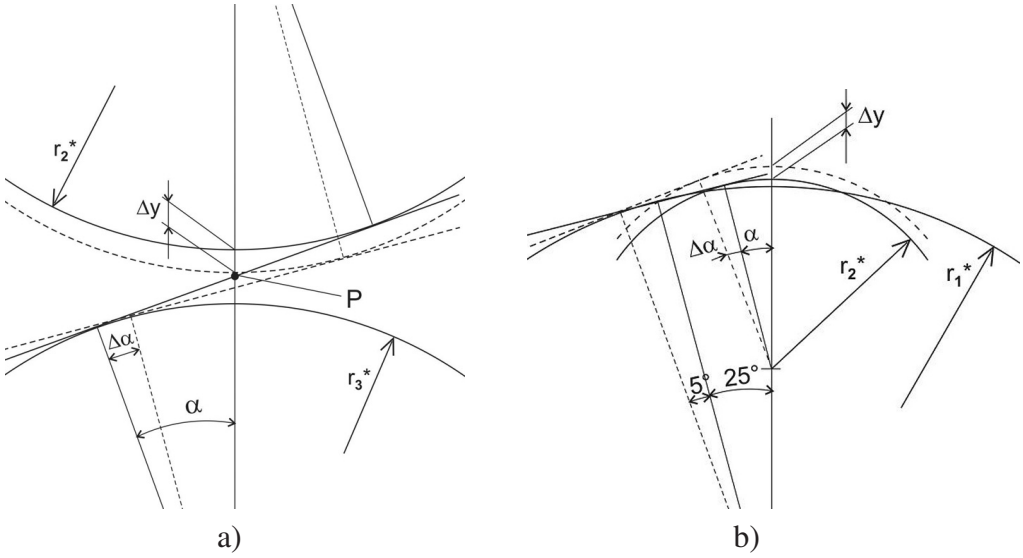

Fig. 3. a) External mesh, b) Internal mesh

The mutual forces in wheels contact at theirs centres approaching Δy are given by the change of pressure angle $\Delta\alpha$, as shown in Fig. 3a by the dashed lines. The radial component of mesh contact force decreases

$$\Delta F = F(\sin(\alpha - |\Delta\alpha|) - \sin(\alpha)) \cong -F\cos(\alpha)\sin(|\Delta\alpha|). \tag{6}$$

The change $\Delta\alpha = 1°$ gives $\Delta F/F = 0.015\,82$. The change of pressure angle $\Delta\alpha$ is connected with the radial shift Δy. The radiuses r_3^*, r_2^* of base circles together with the pressure angle α and its change $\Delta\alpha$ determine this radial shift Δy:

$$\Delta y = \frac{r_3^* + r_2^*}{\cos(\alpha)} - \frac{r_3^* + r_2^*}{\cos(\alpha - |\Delta\alpha|)} \cong \frac{(r_3^* + r_2^*)\sin(\alpha)\sin(|\Delta\alpha|)}{\cos^2(\alpha)}. \tag{7}$$

After substitution of $\sin(|\Delta\alpha|)$ from Eq. (6), we get the relation between the increase of radial force ΔF and the radial shift Δy, i.e. the radial contact stiffness k_r:

$$k_{r32} = \frac{\Delta F}{\Delta y} = \frac{-F\cos^3(\alpha)}{(r_3^* + r_2^*)\sin(\alpha)} = \frac{-F\cos^2(\alpha)}{(r_3 + r_2)\sin(\alpha)}. \tag{8}$$

An interesting property of this radial external mesh stiffness is its negative value.

Similar relations are valid also for the radial contact force between ring and planetary wheel. A situation when the wheel centres approaches Δy is shown in Fig. 3b with dashed lines. The basic difference compared to the previous case is in the internal gearing of the ring wheel. In this tooth system, the pressure angle α increases $\Delta\alpha > 0$ at positive wheels centres approaching Δy. The radial component of mesh contact force increases with increasing Δy

$$\Delta F = F(\sin(\alpha + \Delta\alpha) - \sin(\alpha)) \cong F\cos(\alpha)\sin(\Delta\alpha). \tag{9}$$

The radial contact stiffness k_r of this internal gearing set is positive as opposed to the external gearing set:

$$k_{r21} = \frac{\Delta F}{\Delta y} = \frac{F\cos^3(\alpha)}{(r_1^* - r_2^*)\sin(\alpha)} = \frac{F\cos^2(\alpha)}{(r_1 - r_2)\sin(\alpha)}. \tag{10}$$

The combination of external and internal gearings is a typical property of planetary gearings. The gearing connection between the central sun wheel (3) and the planet (2) is external, whereas between the planet (2) and the ring wheel (1), there is an internal gearing, see Figs. 1 and 4.

Because in planetary gearing is valid $r_3 + r_2 = r_1 - r_2$ and contact forces F_1, F_2 acting on the satellite are approximately the same, then the radial stiffness in external and internal gear contacts at the same pressure angle α have the same absolute value, but opposite signs:

$$k_{r21} = -k_{r32} = k_r. \tag{11}$$

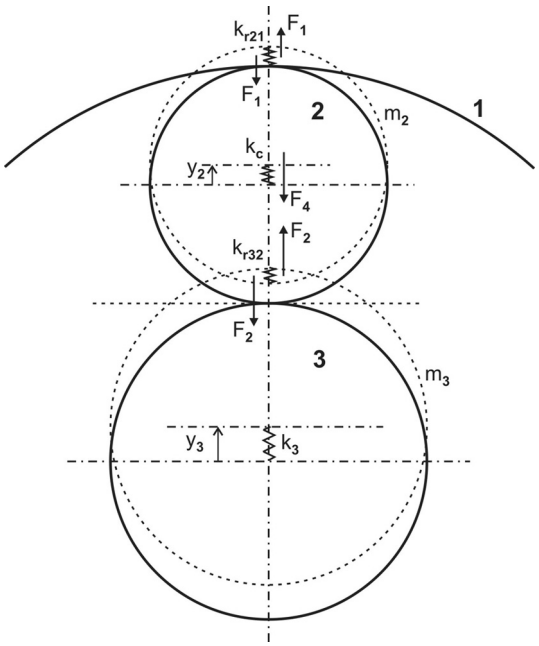

Fig. 4. Vertical motion

The contact stiffness k_r is proportional to the preload, i.e. to the transferring torsion moment. Let be $F = 1\,000$ N and pressure angle $\alpha = 25°(\cos\alpha = 0.906\,3)$. Then the radial contact stiffness k_{r32} in the gear mesh of sun gear (3) ($r_3 = 0.05$ m) with planet gear (2) ($r_2 = 0.1$ m) is

$$k_{r32} = \frac{-1\,000 \cdot 0.906\,3^2}{(0.1 + 0.05) \cdot 0.422\,6} \cong -13\,000\ \mathrm{N/m}. \tag{12}$$

In comparison to the tangential stiffness of gearing, this stiffness is very low, but in same cases it can cause an instability. An example of such case is a radial motion of one planetary branch, scheme of which is shown in Fig. 4.

Planetary gears have several advantages over simple parallel axis gears, for example, the distribution of power flow into several planetary wings enables to increase power density transmission. For uniform distribution of power flow on all planetary wings, in spite of production and assembling errors, the flexible planetary pins and free or very weakly supported sun wheel are used in modern gearing design.

Motion equations of free vertical vibration of this two degree-of-freedom (DOF) system with immobile axes of the ring wheel ($y_1 = 0$), flexible planetary pin (k_c) and very weakly supported sun axes (k_3) are following

$$\begin{aligned} m_3\ddot{y}_3 - k_{r32}(y_3 - y_2) + k_3 y_3 = 0, \\ m_2\ddot{y}_2 + k_{r32}(y_3 - y_2) + k_{r21}y_2 + k_c y_2 = 0. \end{aligned} \tag{13}$$

After using (11), equations (13) can be simplified to

$$\begin{aligned} m_3\ddot{y}_3 - k_r(y_3 - y_2) + k_3 y_3 = 0, \\ m_2\ddot{y}_2 + k_r y_3 + k_c y_2 = 0 \end{aligned} \tag{14}$$

with the determinant

$$\det = \Omega^4 m_2 m_3 - \Omega^2(m_3 k_c + m_2(k_3 - k_r)) + k_c k_3 - k_r(k_c + k_r) = 0. \tag{15}$$

After replacing the mass and stiffness parameters in (15) with their numerical values ($m_2 = 50$ kg, $m_3 = 100$ kg, $k_c = 1.0 \cdot 10^8$ N/m, $k_r = 13\,000$ N/m) and taking several values of the sun wheel stiffness ($k_3 = 0, 5, 10, 15, 20$ kN/m), we get the square of eigenfrequencies Ω^2 [(rad/s)^2] written in Table 1 or simple eigenfrequencies Ω [rad/s] listed in Table 2.

Table 1. Square of eigenfrequencies

k_3 / Eigenfr.^{2}	0 kN/m	5 kN/m	10 kN/m	15 kN/m	20 kN/m
Ω_1^2 [(rad/s)^2]	-520.06	-320.07	-120.07	79.93	279.93
Ω_2^2 [(rad/s)^2]	$2.000 \cdot 10^6$	$2.000 \cdot 10^6$	$2.000 \cdot 10^6$	$2.000 \cdot 10^6$	$2.000 \cdot 10^6$

Table 2. Eigenfrequencies

k_3 / Eigenfr.	0 kN/m	5 kN/m	10 kN/m	15 kN/m	20 kN/m
Ω_1 [rad/s]	22.80i	17.89i	10.96i	8.94	16.73
Ω_2 [rad/s]	1 414.21	1 414.21	1 414.21	1 414.21	1 414.21

The negative radial mesh stiffness k_r in the contact between satellite and free unsupported sun wheel ($k_3 = 0$) leads to unstable gear wings ($\Omega_1^2 = -520.06$ (rad/s)^2). An addition of supporting spring with stiffness $k_3 = 5$ or 10 kN/m to the sun wheel axis decreases the level of instability ($\Omega_1^2 = -320.07$ (rad/s)^2 or $\Omega_1^2 = -120.07$ (rad/s)^2). The stronger spring with stiffness $k_3 = 15$ kN/m reverses instability and the system becomes stable ($\Omega_1^2 = 79.93$ (rad/s)^2) with the eigenfrequency $\Omega_1 = 8.94$ rad/s. The stiffness k_3 strongly influences the lowest eigenfrequency Ω_1 unlike the eigenfrequency Ω_2, which remains constant, roughly independent on k_3, as seen from the last row of Tables 1 and 2.

The graphical representation of these frequency spectrum properties is shown in Fig. 5. The upper graph shows the linear increase of the square of the lower eigenfrequency Ω_1^2 with the increase in stiffness k_3. The value of Ω_1^2 changes its sign at $k_3 = k_r$. The lower graph shows the dependence of eigenfrequency Ω_1 on stiffness k_3. For $k_3 < k_r$, this eigenfrequency has an imaginary value (plotted in dashed lines) and the system is unstable. For $k_3 > k_r$, the imaginary component of eigenfrequency Ω_1 is zero, whereas the real component has an increasing positive value and results in stable oscillation of the central sun wheel.

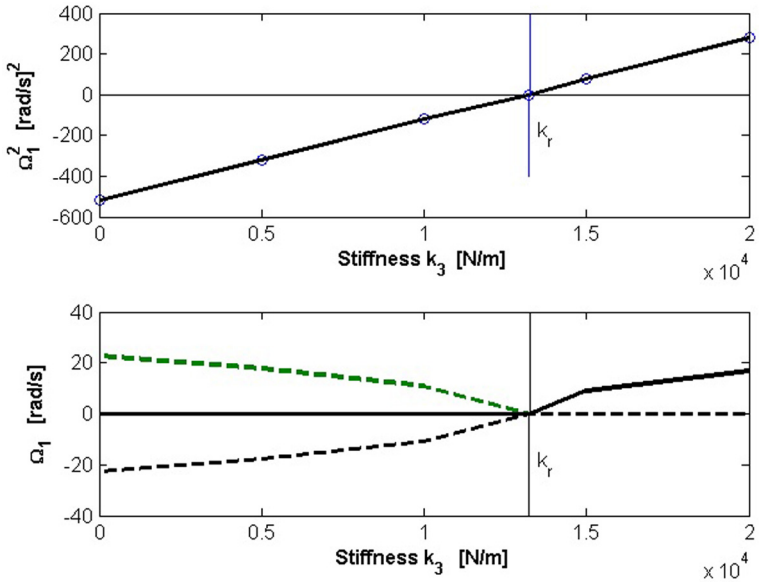

Fig. 5. Eigenfrequencies at variable stiffness k_3

Another situation is in the planetary wheel, which has two contacts. The lower radial contact with sun wheel has stiffness $-k_r$, the upper radial contact with ring wheel is internal and has positive stiffness $+k_r$. These stiffness parameters are in equilibrium and the stable position of planetary wheel is ensured by the positive stiffness k_c of the planetary pin.

The worst stability conditions occur in the two-planet system shown in Fig. 6a, where on the free sun central wheel act two radial forces with negative stiffness. In real planetary gearings with more than two planetary wings, as shown in Fig. 6b, the much higher tangential tooth stiffness from the wings perpendicular to the central wheel's displacement stabilised the entire system and the motion of sun wheel, even if it is free, is also stable.

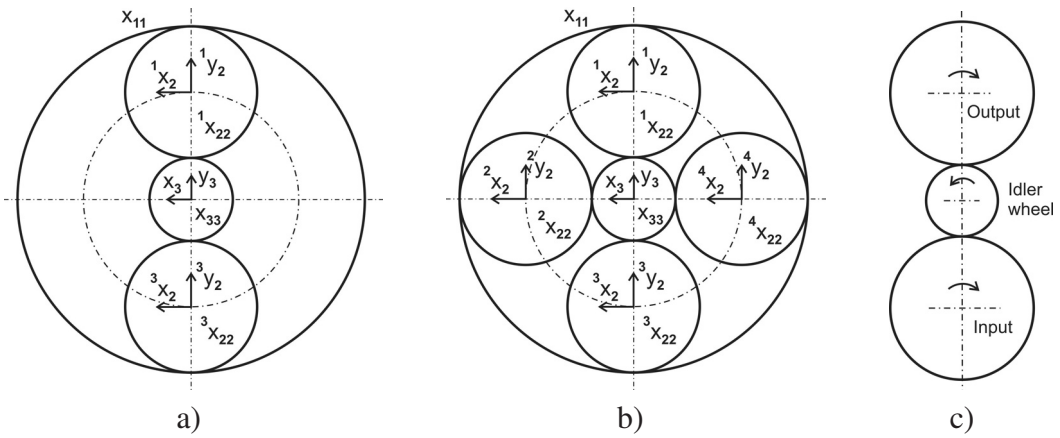

Fig. 6. Free sun central wheels

The instability issue also applies to the idler gear wheel (Fig. 6c) inserted between two other gear wheels to change the direction of rotation of the output shaft. Usually, the stiff pin of this idler wheel ensures sufficient level of stability and no problems occur. However, if there is some clearance in the idler gear bearing, undesirable vibrations can arise.

3. Conclusion

This paper dealt with a phenomenon, which is nearly always neglected in the literature concerning gearing. This phenomenon is the radial stiffness of contacts between gears at change of axes distance. It has been shown that this stiffness depends on gear load, pressure angle and base diameters of contacting gears. The stiffness value is negative for external gearings, and positive for internal gearings. On examples, it has been shown that this radial stiffness is small in comparison with the tangential stiffness, but in some special cases it can cause instability of motion.

Acknowledgements

This work has been elaborated in the frame of the grant project TA04011656.

Reference

[1] Brepta, R., Půst, L., Turek, F., Mechanical vibrations, Sobotales, Prague, 1994. (in Czech)

[2] Cooley, C. G., Parker, R. G., A review of planetary and epicyclic gear dynamics and vibrations research, Applied Mechanics Reviews 66 (4) (2014), doi: 10.1115/1.4027812.

[3] Doležal, Z., Solution of the high-speed planetary gearbox by means of complex dynamic compliance method, Proceedings of the conference Dynamics of Machines, Prague, Liblice, 1977, pp. 85–90. (in Czech)

[4] Hortel, M., Škuderová, A., Planetary differential system – simulation model, Research report Z-1521/14, Institute of Thermomechanics ASCR, 2014. (in Czech)

[5] Ji, D. D., Song, Z. M., Yhang, J., Dynamics in the gear train set in wind turbine, Materials Science Forum 697 (2012) 701–705.

[6] Parker, R. G., A physical explanation for the effectiveness of planet phasing to suppress planetary gear vibration, Journal of Sound and Vibration 236 (4) (2000) 561–573.

[7] Peeters, J., Vandepitte, D., Sas, P., Flexible multi-body model of a three-stage planetary gearbox in a wind turbine, Proceedings of ISMA 2004 – International Conference on Noise and Vibration Engineering, Leuven, Belgium, 2004, pp. 3 923–3 941.

[8] Půst, L., Pešek, L., Radolfová, A., Dynamics of simple planet gearing model, Proceedings of the conference Engineering Mechanics 2015, Svratka, 2015, pp. 246–247.

[9] Yanabe, S., Yoshino, M., Self-centring characteristics of floating sun gear in a star-type planetary gear train, Proceedings of the 10^{th} congress on Theory of Mechanisms and Machines, Oulu, Finland, 1999, pp. 2 386–2 391.

[10] Zeman, V., Internal dynamics of stereo static planetary gearing with herringbone wheels, Strojnícký Časopis 20 (3) (1969) 249–266. (in Czech)

[11] Zhu, C. C., Xu, X. Y., Lim, T. C., Du, X. S., Liu, M. Y., Effect of flexible pin on the dynamic behaviors of wind turbine planetary gear drives, Journal of Mechanical Engineering Science 227(1) (2013) 74–86.